Advances in Applied Mathematics and Mechanics
Adv. Appl. Math. Mech., Vol. **5**, No. 3, pp. 391-406

DOI: 10.4208/aamm.2012.m39
June 2013

Buckling of 2D-FG Cylindrical Shells under Combined External Pressure and Axial Compression

R. Mohammadzadeh[1,*], M. M. Najafizadeh[1] and M. Nejati[2]

[1] *Department of Mechanical Engineering, Islamic Azad University, Arak Branch, Arak, Iran*
[2] *Young Researchers Club, Islamic Azad University, Arak Branch, Arak, Iran*

Received 2 December 2012; Accepted (in revised version) 31 January 2013

Available online 30 April 2013

Abstract. This paper presents the stability of two-dimensional functionally graded (2D-FG) cylindrical shells subjected to combined external pressure and axial compression loads, based on classical shell theory. The material properties of functionally graded cylindrical shell are graded in two directional (radial and axial) and determined by the rule of mixture. The Euler's equation is employed to derive the stability equations, which are solved by GDQ method to obtain the critical mechanical buckling loads of the 2D-FG cylindrical shells. The effects of shell geometry, the mechanical properties distribution in radial and axial direction on the critical buckling load are studied and compared with a cylindrical shell made of 1D-FGM. The numerical results reveal that the 2D-FGM has a significant effect on the critical buckling load.

AMS subject classifications: 74K25, 74G60

Key words: Mechanical buckling, 2D-FG cylindrical shell, combined load, classical shell theory, GDQ method.

1 Introduction

Functionally graded structures are those in which the volume fractions of two or more materials are varied smoothly and continuously as a function of positions along with certain direction(s) of the structure to achieve a required function. These materials were used for the first time by a group of scientists in Sendai, Japan, in 1984 [1,2]. The gradual change of material properties can be proportional to different applications and working environments.

Mechanical Buckling of a circular cylindrical shell, as a major structure, is being studied for a long time. The buckling behavior of structural members made of homogeneous

*Corresponding author.
Email: rmohammadzadeh@ymail.com (R. Mohammadzadeh)

materials subjected to mechanical loads are studied by Brush and Almorth [3]. Vodenitcharova and Ansourian [4] presented the buckling analysis of circular cylindrical shells subjected to a uniform lateral pressure. Based on the first order shear deformation theory (FSDT), Khazaeinejad et al. [5] studied on the buckling of functionally cylindrical shells under external pressure and axial compression.

The most familiar FGM is compositionally graded from one surface to another with a prescribed function. But conventional FGM may not be so effective in some structures since all outer or inner surfaces will have the same composition distributions while in developed machine elements, temperature and load distribution may change in two or more directions [6]. For this reason, we introduced 2D-FGM properties which are dependent bi-directionally. Recently some works have been done on 2D-FGM. Dhaliwal and Singh [7] solved the equations of equilibrium for a non-homogeneous elastic solid under shearing forces. Sobhani Aragh and Hedayati [8] studied the static response and free vibration of two-dimensional functionally graded metal/ceramic open cylindrical shells under various boundary conditions. Pindera and Aboudi studied a coupled higher-order theory for cylindrical structural components with bi-directionally graded microstructures [9]. Also Asgari et al. [10] considered the solution of dynamic analysis of a thick hollow cylinder with finite length made of two-dimensional functionally graded material (2D-FGM) and subjected to the impact of internal pressure.

Numerous methods have been developed and used for studying the buckling of circular cylindrical shells. However, in this study, using the GDQ method, the stability equations and critical buckling loads are obtained. The GDQ method is a global approximate method. In GDQ method the derivative of a function with respect to a coordinate direction can be expressed as a weighted linear sum of all the functional values at all mesh points along that direction and a continuous function can be approximated by high order polynomials in the overall domain [11].

According to the authors' information, there haven't been any investigations on the buckling of 2D-FG cylindrical shells. In this study, the stability of 2D-FG circular cylindrical shells subjected to combined mechanical loads and based on the classical shell theory is presented considering Young's Modulus changes the material in two directional (radial and axial). To express the combination of applied axial compression and external pressure, a load interaction parameter is defined. The critical buckling loads are obtained for variation of the material constitutions, load interaction parameters, aspect ratios and thickness ratios. Comparing studies are presented to validate the present analysis results. Also, the results reveal that the 2D-FGM has significant effect on the critical buckling load.

2 Material and methods

Consider a cylindrical shell made of two directional functionally graded material (2D-FGM) of mean radius R, thickness h, and length L as shown in Figs. 1 and 2. The 2D-FG

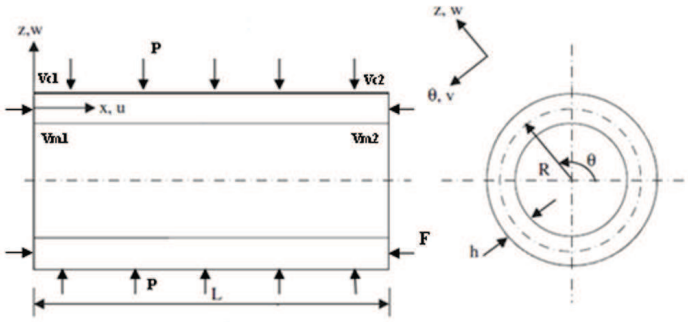

Figure 1: Geometry and coordinate system of a 2D-FG cylindrical shell under combined loads.

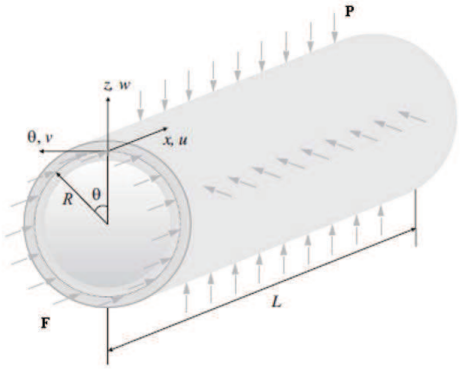

Figure 2: A schematic view of the problem studied.

cylindrical shell is subjected to a uniform external pressure P and an axial compressive load F. Poisson's ratio is assumed to be constant. The displacement components in the x, θ and z direction are denoted by u, v and w, respectively.

We use the Voigt model as the rule of mixture approximation [12] with the volume fraction in the radial and axial directions with predetermined continuous functions. Therefore the volume fraction distribution function of 2D-FG shell can be explained as [10]

$$\begin{aligned} V_{c1} &= \left(\frac{1}{2}+\frac{z}{h}\right)^{n_z}\left(1-\left(\frac{x}{L}\right)^{n_x}\right), & V_{c2} &= \left(\frac{1}{2}+\frac{z}{h}\right)^{n_z}\left(\frac{x}{L}\right)^{n_x}, \\ V_{m1} &= \left(1-\left(\frac{1}{2}+\frac{z}{h}\right)^{n_z}\right)\left(1-\left(\frac{x}{L}\right)^{n_x}\right), & V_{m2} &= \left(1-\left(\frac{1}{2}+\frac{z}{h}\right)^{n_z}\right)\left(\frac{x}{L}\right)^{n_x}. \end{aligned} \tag{2.1}$$

Here subscripts $c1$, $c2$, $m1$ and $m2$ indicates first ceramic, second ceramic, first metal and second metal, respectively and volume fraction indexes, n_x and n_z $(0<n_x, n_z<\infty)$ denotes the material variation profile through the 2D-FG shell axes and thickness, respectively.

The Young's modulus of such shell can be determined as follows

$$E(x,z) = E_{m1}V_{m1}+E_{m2}V_{m2}+E_{c1}V_{c1}+E_{c2}V_{c2}. \tag{2.2}$$

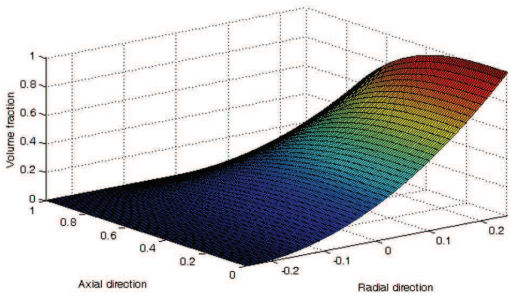

Figure 3: Volume fraction distribution of $c1$.

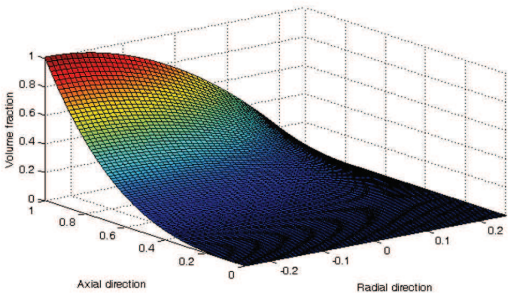

Figure 4: Volume fraction distribution of $m2$.

Here, E_{m1}, E_{m2}, E_{c1} and E_{c2} are the corresponding properties of the first and the second metals and the ceramics, respectively. The material composition variation on each boundary surface is given as:

$$\text{at } x=0,\ z=-\frac{h}{2}:\ V_{c1}=0,\ V_{c2}=0,\ V_{m1}=1,\ V_{m2}=0, \tag{2.3a}$$

$$\text{at } x=0,\ z=+\frac{h}{2}:\ V_{c1}=1,\ V_{c2}=0,\ V_{m1}=0,\ V_{m2}=0, \tag{2.3b}$$

$$\text{at } x=L,\ z=-\frac{h}{2}:\ V_{c1}=0,\ V_{c2}=0,\ V_{m1}=0,\ V_{m2}=1, \tag{2.3c}$$

$$\text{at } x=L,\ z=+\frac{h}{2}:\ V_{c1}=0,\ V_{c2}=1,\ V_{m1}=0,\ V_{m2}=0. \tag{2.3d}$$

According the Eq. (2.1), we may have four states on interaction region:

$$1)\ \text{if } n_x,n_z>1: \qquad V_{m1}>V_{m2}=V_{c1}>V_{c2}, \tag{2.4a}$$

$$2)\ \text{if } 0<n_x,n_z<1: \qquad V_{c2}>V_{c1}=V_{m2}>V_{m1}, \tag{2.4b}$$

$$3)\ \text{if } 0<n_x<1,n_z>1: \qquad V_{m2}>V_{m1}>V_{c2}>V_{c1}, \tag{2.4c}$$

$$4)\ \text{if } 0<n_z<1,n_x>1: \qquad V_{c1}>V_{m1}>V_{c2}>V_{m2}. \tag{2.4d}$$

For example, the volume fraction distributions of two basis materials for the typical values of $n_z=2$ and $n_x=3$ are shown in Figs. 3 and 4. In this case $h=0.5$m and $L=1$m.

The basic constituents of the 2D-FG cylindrical shell are shown in Table 1.

Table 1: Basic Constituents of 2D-FG cylindrical shell.

Constituents	Material	E(Gpa)
$m1$	Ti6Al4V	115
$m2$	Al	70
$c1$	SiC	440
$c2$	Al2O3	380

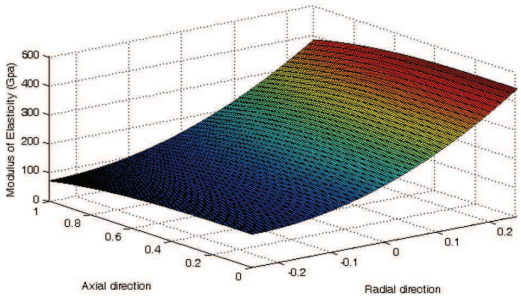

Figure 5: Distribution of modulus of elasticity through the cylinder.

The distribution of one typical property, modulus of elasticity, through the cylinder are shown in Fig. 5.

The nonlinear strain-displacement relations are [3]

$$\overline{\varepsilon}_{xx}=u_{0,x}+\frac{1}{2}w_{0,x}^2,\quad \overline{\varepsilon}_{\theta\theta}=\frac{v_{0,\theta}+w}{R}+\frac{1}{2R^2}w_{0,\theta}^2,\quad \overline{\gamma}_{x\theta}=\frac{u_{0,\theta}}{R}+v_{0,x}+\frac{w_{0,x}w_{0,\theta}}{R},\tag{2.5}$$

where $\overline{\varepsilon}_{xx}$ and $\overline{\varepsilon}_{\theta\theta}$ are the normal strains and $\overline{\gamma}_{x\theta}$ is the shear strain. The classical shell theory used in the present study is based on the following displacement fields [13]

$$u(x,\theta,z)=u_0(x,\theta)-z\frac{\partial w}{\partial x},\quad v(x,\theta,z)=v_0(x,\theta)-\frac{z}{R}\frac{\partial w}{\partial \theta},\quad w(x,\theta,z)=w_0(x,\theta),\tag{2.6}$$

where $u_0(x,\theta)$, $v_0(x,\theta)$ and $w_0(x,\theta)$ are the middle surface displacement $(z=0)$ of the shell, and $-\frac{\partial w}{\partial x}$ and $-\frac{1}{R}\frac{\partial w}{\partial \theta}$ describe the rotations about θ- and x-axes, respectively. Substituting Eq. (2.6) in the relations (2.5) gives the kinematic relations as

$$\left\{\begin{array}{c}\varepsilon_{xx}\\ \varepsilon_{\theta\theta}\\ \gamma_{x\theta}\end{array}\right\}=\left\{\begin{array}{c}\overline{\varepsilon}_{xx}\\ \overline{\varepsilon}_{\theta\theta}\\ \overline{\gamma}_{x\theta}\end{array}\right\}+z\left\{\begin{array}{c}\kappa_x\\ \kappa_\theta\\ 2\kappa_{x\theta}\end{array}\right\},\qquad \left\{\begin{array}{c}\kappa_x\\ \kappa_\theta\\ \kappa_{x\theta}\end{array}\right\}=\left\{\begin{array}{c}-w_{0,xx}\\ -\dfrac{w_{0,\theta\theta}}{R^2}\\ -\dfrac{w_{0,x\theta}}{R}\end{array}\right\}.\tag{2.7}$$

Using Hook's law the stress-strain relations are given as follow

$$\sigma_{xx}=\frac{E(x,z)}{1-v^2}(\varepsilon_{xx}+v\varepsilon_{\theta\theta}),\quad \sigma_{\theta\theta}=\frac{E(x,z)}{1-v^2}(\varepsilon_{\theta\theta}+v\varepsilon_{xx}),\quad \tau_{x\theta}=\frac{E(x,z)}{2(1+v)}\gamma_{x\theta}.\tag{2.8}$$

The constitutive relations of 2D-FG cylindrical shells are expressed as:

$$\left\{\begin{array}{c}N_x\\ M_x\end{array}\right\}=\left\{\begin{array}{c}K_1h\\ K_2h^2\end{array}\right\}(\overline{\varepsilon}_{xx}+v\overline{\varepsilon}_{\theta\theta})+\left\{\begin{array}{c}K_2h^2\\ K_3h^3\end{array}\right\}(\kappa_x+v\kappa_\theta),\tag{2.9a}$$

$$\left\{\begin{array}{c}N_\theta\\ M_\theta\end{array}\right\}=\left\{\begin{array}{c}K_1h\\ K_2h^2\end{array}\right\}(\overline{\varepsilon}_{\theta\theta}+v\overline{\varepsilon}_{xx})+\left\{\begin{array}{c}K_2h^2\\ K_3h^3\end{array}\right\}(\kappa_\theta+v\kappa_x),\tag{2.9b}$$

$$\left\{\begin{array}{c}N_{x\theta}\\ M_{x\theta}\end{array}\right\}=\frac{1-v}{2}\left(\left\{\begin{array}{c}K_1h\\ K_2h^2\end{array}\right\}\overline{\gamma}_{x\theta}+\left\{\begin{array}{c}K_2h^2\\ K_3h^3\end{array}\right\}\kappa_{x\theta}\right),\tag{2.9c}$$

where K_1, K_2 and K_3 are defined as

$$K_1(x,z)=\frac{\left(\left(E_{m1}+\frac{E_3}{n_z+1}\right)+\left(\frac{x}{L}\right)^{n_x}\left(E_2+\frac{E_1}{n_z+1}\right)\right)}{1-v^2}, \tag{2.10a}$$

$$K_2(x,z)=\frac{\left(\left(E_3+E_1\left(\frac{x}{L}\right)^{n_x}\right)\left(\frac{1}{n_z+2}-\frac{0.5}{n_z+1}\right)\right)}{1-v^2}, \tag{2.10b}$$

$$K_3\left(x,z\right)=\frac{\left(\frac{E_{m1}+E_2\left(\frac{x}{L}\right)^{n_x}}{12}+\left(E_3+E_1\left(\frac{x}{L}\right)^{n_x}\right)\left(\frac{1}{n_z+3}-\frac{1}{n_z+2}+\frac{0.25}{n_z+1}\right)\right)}{1-v^2}. \tag{2.10c}$$

In which we have

$$E_1=E_{m1}-E_{m2}-E_{c1}+E_{c2},\quad E_2=E_{m2}-E_{m1},\quad E_3=E_{c1}-E_{m1}. \tag{2.11}$$

The stress resultants are defined in the following form

$$\begin{aligned}&(N_x,M_x)=\int_{-\frac{h}{2}}^{+\frac{h}{2}}\sigma_{xx}(1,z)dz,\qquad (N_\theta,M_\theta)=\int_{-\frac{h}{2}}^{+\frac{h}{2}}\sigma_{\theta\theta}(1,z)dz,\\&(N_{x\theta},M_{x\theta})=\int_{-\frac{h}{2}}^{+\frac{h}{2}}\tau_{x\theta}(1,z)dz.\end{aligned} \tag{2.12}$$

By using the variation approach and Euler equations, the equilibrium equations of 2D-FG cylindrical shells Under Combined External Pressure and Axial Compression based on the classical shell theory are derived as follows [3]

$$\begin{aligned}&RN_{x,x}+N_{x\theta,\theta}=0,\qquad RN_{x\theta,x}+N_{\theta,\theta}=0,\\&RM_{x,xx}+2M_{x\theta,x\theta}+\frac{1}{R}M_{\theta,\theta\theta}-N_\theta+RN_xw_{,xx}+2N_{x\theta}w_{,x\theta}+\frac{1}{R}N_\theta w_{,\theta\theta}=-PR.\end{aligned} \tag{2.13}$$

The Euler's principle is employed to derive the stability equations [3]. By using Taylor series we can expand V(the total potential energy of the shell) about the equilibrium state as follows

$$\Delta V=\delta V+\frac{1}{2}\delta^2V+\frac{1}{6}\delta^3V+\cdots, \tag{2.14}$$

δV (the first variation) is related to the equilibrium state. The second variation (δ^2V) is the state of stability of the original configuration of the shell in the neighborhood of the equilibrium state. The condition $\delta^2V=0$ is utilized to obtain the stability equations for buckling problems [3]. Supposing that u_0, v_0 and w_0 are the displacements of the equilibrium states, the displacement components of a neighboring stable state differ by u_1, v_1

and w_1 with respect to the equilibrium state. Therefore the displacement components of a neighboring state are

$$u=u_0+u_1,\quad v=v_0+v_1,\quad w=w_0+w_1. \tag{2.15}$$

Similarly, the stress resultants of a neighboring state are probably associated with the equilibrium state as

$$(N_x,M_x)=(N_{x0},M_{x0})+(N_{x1},M_{x1}), \tag{2.16a}$$
$$(N_\theta,M_\theta)=(N_{\theta0},M_{\theta0})+(N_{\theta1},M_{\theta1}), \tag{2.16b}$$
$$(N_{x\theta},M_{x\theta})=(N_{x\theta0},M_{x\theta0})+(N_{x\theta1},M_{x\theta1}). \tag{2.16c}$$

The superscript 1 refers to the state of stability and the superscript 0 refers to the state of equilibrium. In addition, the nonlinear terms with superscript 1 are ignored because they are too small compared with the linear terms. Upon substituting Eq. (2.15) and (2.16) in Eq. (2.13); the stability equations for 2D-FG cylindrical shells under combined mechanical loading can be obtained by the means of Euler equations [3] as follow

$$\begin{aligned}&RN_{x1,x}+N_{x\theta1,\theta}=0,\qquad RN_{x\theta1,x}+N_{\theta1,\theta}=0,\\&RM_{x1,xx}+2M_{x\theta1,x\theta}+\frac{1}{R}M_{\theta1,\theta\theta}-N_{\theta1}+RN_{x0}w_{1,xx}+2N_{x\theta0}w_{1,x\theta}+\frac{1}{R}N_{\theta0}w_{1,\theta\theta}=0.\end{aligned} \tag{2.17}$$

We can rewrite the stability equations in the form of displacements as follow:

$$\begin{aligned}&\frac{\partial}{\partial x}K_1(x,z)h(R^2u_{1,x}+\upsilon R(v_{1,\theta}+w_1))+\frac{\partial}{\partial x}K_2(x,z)h^2(-R^2w_{1,xx}-\upsilon w_{1,\theta\theta})\\&\quad+K_1(x,z)h\left(R^2u_{1,xx}+\frac{1-\upsilon}{2}u_{1,\theta\theta}+R\left(\frac{1+\upsilon}{2}v_{1,x\theta}+\upsilon w_{1,x}\right)\right)\\&\quad+K_2(x,z)h^2(-R^2w_{1,xxx}-w_{1,x\theta\theta})=0,\end{aligned} \tag{2.18a}$$

$$\begin{aligned}&\frac{\partial}{\partial x}K_1(x,z)h\left(\frac{1-\upsilon}{2}(R^2u_{1,\theta}+R^3v_{1,x})\right)+\frac{\partial}{\partial x}K_2(x,z)h^2(-(1-\upsilon)R^2w_{1,x\theta})\\&\quad+K_1(x,z)h\left(\frac{1+\upsilon}{2}R^2u_{1,x\theta}+\frac{1-\upsilon}{2}R^3v_{1,xx}+R(v_{1,\theta\theta}+w_{1,\theta})\right)\\&\quad+K_2(x,z)h^2(-R^2w_{1,xx\theta}-w_{1,\theta\theta\theta})=0,\end{aligned} \tag{2.18b}$$

$$\begin{aligned}&\frac{\partial^2}{\partial x^2}K_2(x,z)h^2(R^4u_{1,x}+\upsilon R^3(v_{1,\theta}+w_1))+\frac{\partial^2}{\partial x^2}K_3(x,z)h^3(-R^4w_{1,xx}-\upsilon R^2w_{1,\theta\theta})\\&\quad+\frac{\partial}{\partial x}K_2(x,z)h^2(2R^4u_{1,xx}+2\upsilon R^3w_{1,x}+(1-\upsilon)R^2u_{1,\theta\theta}+(1+\upsilon)R^3v_{1,x\theta})\\&\quad+\frac{\partial}{\partial x}K_3(x,z)h^3(-2R^4w_{,xxx}-2R^2w_{1,x\theta\theta})\\&\quad+K_2(x,z)h^2(R^4u_{1,xxx}+2\upsilon R^3w_{1,xx}+R^2u_{1,x\theta\theta}+R^3v_{1,xx\theta}+R(v_{1,\theta\theta\theta}+2w_{1,\theta\theta}))\\&\quad+K_3(x,z)h^3(-R^4w_{1,xxxx}-2R^2w_{1,xx\theta\theta}-w_{1,\theta\theta\theta\theta})-K_1(x,z)h(R^2(w_1+v_{1,\theta})+\upsilon R^3u_{1,x})\\&\quad+R^4N_{x0}w_{1,xx}+2R^3N_{x\theta0}w_{1,x\theta}+R^2N_{\theta0}w_{1,\theta\theta}=0.\end{aligned} \tag{2.18c}$$

3 Theory/calculation

In this section, by using the GDQ method, the critical buckling of 2D-FG cylindrical shells under combined mechanical loads are obtained. Under the assumed loading, the prebuckling deformation of the shell is axisymmetric. Also the $N_{x\theta 0}=0$ (because there is not any torsional loading). Furthermore the other prebuckling mechanical forces are obtained from Hook's law and also the linear membrane equilibrium equations

$$N_{x0}=-\frac{F}{2\pi R},\qquad N_{\theta 0}=-PR. \tag{3.1}$$

With respect to the above remarks, we can rewrite Eq. (2.17) as follow

$$\begin{aligned}&RN_{x1,x}+N_{x\theta 1,\theta}=0,\qquad RN_{x\theta 1,x}+N_{\theta 1,\theta}=0,\\&R^2M_{x1,xx}+2RM_{x\theta 1,x\theta}+M_{\theta 1,\theta\theta}-RN_{\theta 1}-\eta PR^3w_{1,xx}+PRw_{1,\theta\theta}=0.\end{aligned} \tag{3.2}$$

The nondimensional load parameter η is defined to express the combination of the applied axial compression and external pressure [5]

$$\eta=\frac{F}{2\pi R^2P}. \tag{3.3}$$

The 2D-FG cylindrical shell is assumed to have simply supports on both ends. Therefore the boundary conditions are defined as

$$\text{at } x=0,L:\ w_1=v_1=M_{x1}=N_{x1}=0. \tag{3.4}$$

Generally, it's rather difficult to get an analytical solution of Eq. (2.18) due to the nature of bi-directional non-homogeneity. In the present study differential quadrature method is employed to obtain the critical buckling loads of 2D-FG cylindrical shells. This is a fast-computing approach for partial differential equations with variable coefficients which provides accurate results [11].

According to Generalized Differential Quadrature Method (GDQM), the nth-order derivative of the solution function $f(x)$ at grid point "i" can be written as [11]

$$f_x^{(n)}(x_i)=\sum_{j=1}^{N}C_{ij}^{(n)}f(x_j),\qquad i=1,2,\cdots,N,\quad n=1,2,\cdots,N-1, \tag{3.5a}$$

$$C_{ij}^{(1)}=\frac{M^{(1)}(x_i)}{(x_i-x_j)M^{(1)}(x_j)},\qquad j=1,2,\cdots,N,\quad i\neq j, \tag{3.5b}$$

$$M^{(1)}(x_i)=\prod_{\substack{j=1\\ j\neq 1}}^{N}(x_i-x_j), \tag{3.5c}$$

$$C_{ij}^{(n)}=n\left(C_{ii}^{(n-1)}C_{ij}^{(1)}-\frac{C_{ij}^{(n-1)}}{x_i-x_j}\right),\quad i,j=1,2,\cdots,N,\quad i\neq j,\quad n=2,3,\cdots,N-1, \tag{3.5d}$$

$$C_{ii}^{(n)}=-\sum_{\substack{j=1\\ i\neq j}}^{N}C_{ij}^{(n)},\qquad i=1,2,\cdots,N,\qquad n=1,2,\cdots,N-1. \tag{3.5e}$$

In this equation $C_{ij}^{(n)}$ are the weighting coefficients of n-th order derivative and N is the total number of grid points. It has been shown that the Chebyshev-Gauss-Lobatto grid point distribution have great convergence and stability. Therefore the present study applies Chebyshev-Gauss-Lobatto grid points positions in one dimensional form are given by [11]

$$x_i=\frac{l}{2}\left\{1-\cos\left(\frac{i-1}{N-1}\right)\pi\right\},\quad i=1,2,\cdots,N. \tag{3.6}$$

To solve the stability equations, the displacement fields u, v and w are defined as products of unknown functions along the axial direction and known trigonometric functions along with the circumferential directions as follow [14]

$$u_1(x,\theta)=U_1(x)\cos n\theta,\quad v_1(x,\theta)=V_1(x)\sin n\theta,\quad w_1(x,\theta)=W_1(x)\cos n\theta. \tag{3.7}$$

Here n is the wave number in the θ-direction and $U_1(x)$, $V_1(x)$ and $W_1(x)$ are the unknown axial functions.

This approach uses the basis of the quadrature method in deriving the derivatives of a function. It follows that the partial derivative of a function with respect to a space variable can be approximated by a weighted linear combination of functional values at some intermediate points in that variable [11].

Substituting Eq. (3.7) in Eq. (2.18) and using GDQ method, the buckling equations are derived

$$\begin{aligned}&\frac{\partial}{\partial x}K_1(x,z)h\left(R^2\sum_{k=1}^{n}C_{ik}^{(1)}U_{1k}+vR(nV_{1i}+W_{1i})\right)+\frac{\partial}{\partial x}K_2(x,z)h^2\left(-R^2\sum_{k=1}^{n}C_{ik}^{(2)}W_{1k}+vn^2W_{1i}\right)\\&\quad+K_1(x,z)h\left(R^2\sum_{k=1}^{n}C_{ik}^{(2)}U_{1k}-\frac{1-v}{2}n^2U_{1i}+R\left(\frac{1+v}{2}n\sum_{k=1}^{n}C_{ik}^{(1)}V_{1k}+v\sum_{k=1}^{n}C_{ik}^{(1)}W_{1k}\right)\right)\\&\quad+K_2(x,z)h^2\left(-R^2\sum_{k=1}^{n}C_{ik}^{(3)}W_{1k}+n^2\sum_{k=1}^{n}C_{ik}^{(1)}W_{1k}\right)=0,\end{aligned} \tag{3.8a}$$

$$\begin{aligned}&\frac{\partial}{\partial x}K_1(x,z)h\left(\frac{1-v}{2}\left(R^2nU_{1i}+R^3\sum_{k=1}^{n}C_{ik}^{(1)}V_{1k}\right)\right)+\frac{\partial}{\partial x}K_2(x,z)h^2\left((1-v)R^2n\sum_{k=1}^{n}C_{ik}^{(1)}W_{1k}\right)\\&\quad+K_1(x,z)h\left(-\frac{1+v}{2}R^2n\sum_{k=1}^{n}C_{ik}^{(1)}U_{1k}+\frac{1-v}{2}R^3\sum_{k=1}^{n}C_{ik}^{(2)}V_{1k}-R(n^2V_{1i}+nW_{1i})\right)\\&\quad+K_2(x,z)h^2\left(R^2n\sum_{k=1}^{n}C_{ik}^{(2)}W_{1k}-n^3W_{1i}\right)=0,\end{aligned} \tag{3.8b}$$

$$\frac{\partial^2}{\partial x^2}K_2(x,z)h^2\Big(R^4\sum_{k=1}^{n}C_{ik}^{(1)}U_{1k}+vR^3(nV_{1i}+W_{1i})\Big)+\frac{\partial^2}{\partial x^2}K_3(x,z)h^3\Big(-R^4\sum_{k=1}^{n}C_{ik}^{(2)}W_{1k}+vR^2n^2W_{1i}\Big)$$
$$+\frac{\partial}{\partial x}K_2(x,z)h^2\Bigg(2R^4\sum_{k=1}^{n}C_{ik}^{(2)}U_{1k}+vR^3\Big(n\sum_{k=1}^{n}C_{ik}^{(1)}V_{1k}+2\sum_{k=1}^{n}C_{ik}^{(1)}W_{1k}\Big)$$
$$+\Big(-(1-v)R^2n^2U_{1i}+R^3n\sum_{k=1}^{n}C_{ik}^{(1)}V_{1k}\Big)\Bigg)+\frac{\partial}{\partial x}K_3(x,z)h^3\Big(-2R^4\sum_{k=1}^{n}C_{ik}^{(3)}W_{1k}+2R^2n^2\sum_{k=1}^{n}C_{ik}^{(1)}W_{1k}\Big)$$
$$+K_2(x,z)h^2\Bigg(R^4\sum_{k=1}^{n}C_{ik}^{(3)}U_{1k}+2vR^3\sum_{k=1}^{n}C_{ik}^{(2)}W_{1k}-R^2n^2\sum_{k=1}^{n}C_{ik}^{(1)}U_{1k}+R^3n\sum_{k=1}^{n}C_{ik}^{(2)}V_{1k}$$
$$+R(-n^3V_{1i}-2n^2W_{1i})\Bigg)+K_3(x,z)h^3\Big(-R^4\sum_{k=1}^{n}C_{ik}^{(4)}W_{1k}+2R^2n^2\sum_{k=1}^{n}C_{ik}^{(2)}W_{1k}-n^4W_{1i}\Big)$$
$$-K_1(x,z)h\Big(R^2(W_{1i}+nV_{1i})+vR^3\sum_{k=1}^{n}C_{ik}^{(1)}U_{1k}\Big)-PR^3\Big(R^2\eta\sum_{k=1}^{n}C_{ik}^{(2)}W_{1k}-n^2W_{1i}\Big)=0. \tag{3.8c}$$

In order to carry out the analysis, the domain and the boundary degrees of freedom are separated, and in vector forms they are denoted as (d) and (b), respectively. Based on this definition, the matrix form of the stability equations and the related boundary conditions take the following form:

$$\begin{bmatrix}[A_{bb}] & [A_{bd}]\\ [A_{db}] & [A_{dd}]\end{bmatrix}\begin{Bmatrix}\{X_b\}\\ \{X_d\}\end{Bmatrix}=0. \tag{3.9}$$

Here $\{X_b\}$ and $\{X_d\}$ are as follow:

$$\{X_b\}=\{\{X_{xb}\},\{X_{\theta b}\},\{X_{zb}\}\}^T,\qquad \{X_d\}=\{\{X_{xd}\},\{X_{\theta d}\},\{X_{zd}\}\}^T. \tag{3.10}$$

In relations (3.9) and (3.10), subscripts (b) and (d) correspond to the displacement vectors at the boundaries and domain of the shell, respectively. Eliminating the boundary degrees of freedom, this equation becomes:

$$[A]\{X_d\}=\{0\}, \tag{3.11}$$

where

$$[A]=[A_{dd}]-[A_{db}][A_{bb}]^{-1}[A_{bd}]. \tag{3.12}$$

By setting the determinant of $[A]$ equal to zero to obtain the non-zero solution and optimizing the resulting in terms of half-wave numbers, the critical buckling loads can be obtained.

4 Results and discussions

In this section, with the usage of the classical shell theory [3] and the GDQ method, numerical results have been obtained for different types of combined loadings. For the

Table 2: Comparison of the buckling loads ($P_{cr}\times 104$Mpa, $E=200$GPa, $v=0.3$ and $R/h=300$).

L/R	Shen	Sofiyev	Khazaeinejad	Present study
0.5	2761.397	2769.014	2767.438	2769.014
1	1272.597	1273.504	1273.129	1273.504
2	611.7448	611.7994	611.7016	611.7994
3	402.6016	412.6221	412.5655	412.6221
5	239.0987	239.4282	239.4109	239.4282

Table 3: Comparison of the buckling loads (Mpa) $v=0.3$, $\eta=0$, $R=0.5$m).

L/R	$L/R=0.01$		$L/R=0.02$		$L/R=0.05$	
	Rahmani	Present	Rahmani	Present	Rahmani	Present
1	3.0004	3.0004	17.8708	17.8707	202.7329	202.7127
2	1.3879	1.3879	8.0777	8.0778	84.6642	84.6641
4	0.6934	0.6933	4.0482	4.0483	39.6455	39.6455
8	0.3308	0.3308	2.0975	2.0976	18.8575	18.8576

Table 4: The convergence of the critical buckling load of 2D-FG cylindrical shell.

L/R	$N=5$	$N=7$	$N=9$	$N=11$	$N=13$	$N=15$
1	2.9163	3.0625	3.0006	3.0004	3.0004	3.0004
2	1.3707	1.3890	1.3872	1.3880	1.3880	1.3880
4	0.6839	0.6937	0.6934	0.6934	0.6934	0.6934
8	0.3275	0.3309	0.3308	0.3308	0.3308	0.3308

given values of the power law indexes n_x and n_z, the radius to the thickness ratio R/h, the length to the radius ratio L/R, the values of the circumferential wave numbers may be chosen by the trial giving the smallest value of buckling load. These values are obtained by an optimization program. Poisson's ratio is assumed to be constant 0.3. The boundary conditions along with the edges at $x=0$ and $x=L$ are considered to be simply supported. To verify the formulations, the critical buckling load of a simply supported isotropic cylindrical shell under uniform external pressure $(\eta=0)$ are compared with those reported by Shen [15], Sofiyev [16] and Khazaeinejad [5] in Table 2. An excellent agreement can be seen between these results therefore, confirming the accuracy of present work.

The shell thickness is set to be 0.001m. As a second example consider Table 3. The Table exhibits the comparison of the critical buckling load under lateral pressure for FG cylindrical shell and based on the classical shell theory, between the present solution and those which are reported by Rahmani [17]. The shell is made of alumina and Steel with the modulus of elasticity 380Gpa and 200Gpa, respectively. From Table 3, it is seen that there is a very good agreement between these results confirming the accuracy of the present work.

From Table 4, it can be noticed that there is a rather significant differences between $N=5$ (mesh grid) and $N=7$ when the answers arrive to the relative convergence. From

Table 5: Variation of critical buckling loads (Mpa) against thickness ratio and power law index for $L/R=5$.

n_x	n_z	η	$R/h=5$	$R/h=10$	$R/h=50$	$R/h=100$
1	0	-1	1791.093	292.710	4.761	0.798
		0	1613.990	263.799	4.552	0.779
		0.5	1537.905	251.384	4.454	0.769
		1	1468.635	240.083	4.361	0.760
1	0.5	-1	1211.011	202.662	3.308	0.545
		0	1091.115	182.661	3.162	0.532
		0.5	1039.598	174.074	3.094	0.525
		1	992.690	166.258	3.029	0.519
1	1	-1	965.338	162.871	2.664	0.436
		0	864.905	146.784	2.547	0.425
		0.5	828.562	139.877	2.492	0.420
		1	791.098	133.591	2.439	0.415
1	5	-1	664.538	107.461	1.745	0.295
		0	598.139	96.827	1.668	0.288
		0.5	569.512	92.262	1.632	0.284
		1	543.346	88.108	1.598	0.281

Table 6: Variation of critical buckling loads (Mpa) against thickness ratio and power law index for $L/R=10$.

n_x	n_z	η	$R/h=5$	$R/h=10$	$R/h=50$	$R/h=100$
1	0	-1	1135.721	167.535	2.511	0.403
		0	1023.585	163.372	2.449	0.399
		0.5	975.428	161.364	2.419	0.396
		1	931.599	159.403	2.390	0.394
1	0.5	-1	812.793	112.433	1.768	0.273
		0	732.524	109.626	1.725	0.271
		0.5	698.054	108.272	1.704	0.269
		1	666.680	106.948	1.683	0.268
1	1	-1	662.645	89.261	1.432	0.218
		0	597.212	87.018	1.397	0.216
		0.5	569.113	85.935	1.380	0.215
		1	543.539	84.875	1.363	0.213
1	5	-1	409.186	62.188	0.914	0.149
		0	368.745	60.581	0.891	0.148
		0.5	351.381	59.801	0.880	0.147
		1	335.758	59.035	0.870	0.146

$N=9$ onwards there aren't any significant differences so for any $N\geq 11$ the answers for critical buckling arrive to the best convergence.

The 2D-FGM shell is made from Ti6Al4V/Al/SiC/Al2O3 which their Young's modulus is given in Table 1. The variations of the critical buckling load of 2D-FG cylindrical shells versus the power law indexes n_x and n_z, the thickness ratios R/h, and the aspect ratios L/R under different types of combined loadings are listed in Tables 5-8. It is ob-

Table 7: Variation of critical buckling loads (Mpa) against thickness ratio and power law index for $L/R=20$.

n_x	n_z	η	$R/h=5$	$R/h=10$	$R/h=50$	$R/h=100$
1	0	-1	371.845	64.768	1.300	0.192
		0	362.658	63.170	1.292	0.190
		0.5	358.232	62.400	1.288	0.190
		1	353.913	61.648	1.284	0.189
1	0.5	-1	252.243	45.095	0.875	0.131
		0	246.006	43.982	0.869	0.130
		0.5	243.001	43.445	0.867	0.130
		1	240.069	42.922	0.864	0.129
1	1	-1	201.255	36.362	0.696	0.105
		0	196.275	35.464	0.691	0.104
		0.5	193.875	35.031	0.689	0.104
		1	191.533	34.609	0.687	0.104
1	5	-1	137.843	23.713	0.483	0.071
		0	134.415	23.127	0.480	0.070
		0.5	132.763	22.844	0.478	0.070
		1	131.150	22.569	0.477	0.070

Table 8: Variation of critical buckling loads (Mpa) against thickness ratio and power law index for $L/R=50$.

n_x	n_z	η	$R/h=5$	$R/h=10$	$R/h=50$	$R/h=100$
1	0	-1	302.932	38.516	0.431	0.102
		0	301.448	38.359	0.429	0.101
		0.5	300.685	38.281	0.428	0.101
		1	299.904	38.203	0.428	0.101
1	0.5	-1	201.652	25.765	0.298	0.073
		0	200.563	25.657	0.296	0.072
		0.5	200.001	25.604	0.296	0.072
		1	199.425	25.551	0.295	0.072
1	1	-1	158.973	20.408	0.239	0.059
		0	158.029	20.321	0.238	0.059
		0.5	157.541	20.277	0.238	0.059
		1	157.042	20.234	0.237	0.059
1	5	-1	109.723	14.199	0.158	0.037
		0	108.890	14.131	0.158	0.037
		0.5	108.459	14.097	0.158	0.036
		1	108.016	14.063	0.157	0.036

served that the buckling load is decreased by increasing the thickness ratio R/h, same as increasing in the aspect ratio L/R. The difference between the results for $R/h=10$ and $R/h=100$ is approximately 100%. For $L/R=10$ and $L/R=50$, the difference is about 75%.

The graphs of the dependency of the critical buckling loads and non-homogenous cylindrical shells on the material gradients are shown in Figs. 6 and 7. For 2D-FG shell,

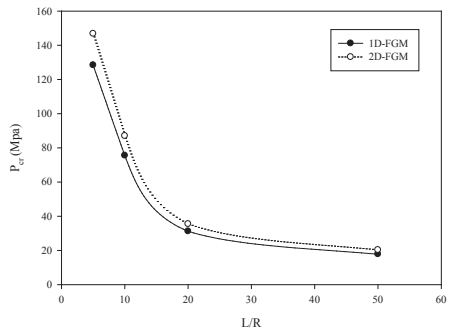

Figure 6: The comparison of the critical buckling loads for 1D-FG and 2D-FG cylindrical shells with $R/h=10$.

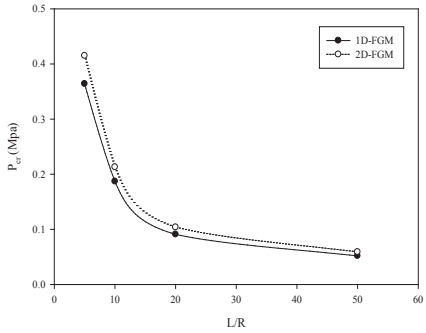

Figure 7: The comparison of the critical buckling loads for 1D-FG and 2D-FG cylindrical shells with $R/h=100$.

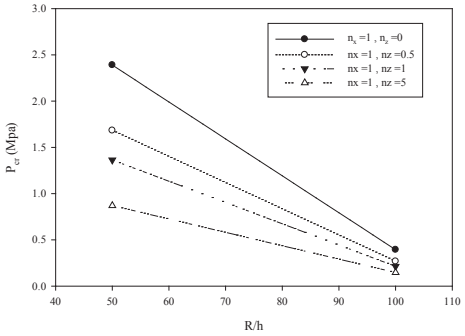

Figure 8: The effect of power law indexes on the critical buckling loads of a 2D-FG cylindrical shells versus R/h ratio for the various power law indexes and $L/R=10$.

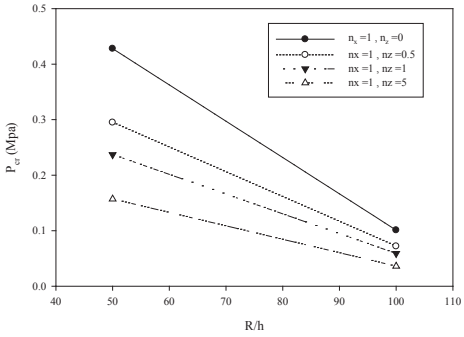

Figure 9: The effect of power law indexes on the critical buckling loads of a 2D-FG cylindrical shells versus R/h ratio for the various power law indexes and $L/R=50$.

the critical buckling loads are increased more than the other type. The critical loads are decreased when increasing L/R ratio.

It is also found that the critical buckling loads are affected by increasing the R/h ratio. For variations of R/h ratio from 10 to 100, the critical buckling load decreases almost 100% in all the cases.

It is also seen from Figs. 8 and 9 that via increasing the power law index n_z from 0 to 5, when $n_x=1$, the critical buckling loads are decreased. This decrease is about 46% for $n_x=1$, $n_z=0.5$ and $n_x=1$, $n_z=5$. It is evident that by increasing L/R ratio from 10 to 50 the values of critical buckling loads are decreased.

Moreover and as it can be seen in Fig. 10, by changing the magnitude and the load parameter η, the critical buckling loads are decreased. As expected, the critical buckling load value of the shell for $\eta=-1$ is higher than the others. The critical buckling load reaches maximum value for lower value of parameter η.

The results confirm that the buckling characteristics are significantly influenced by the variation of the power law indexes, load parameters, thickness ratios, and aspect ratios.

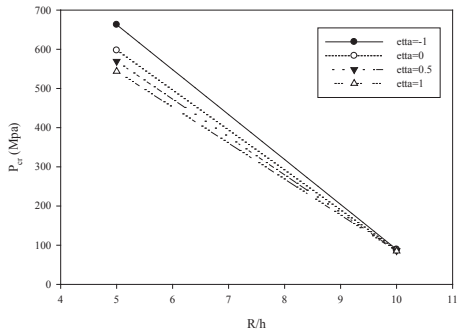

Figure 10: The effect of the load parameter (η) on the critical buckling loads of a 2D-FG cylindrical shells versus R/h ratio for various loads parameter.

5 Conclusions

In the present article, the equilibrium and stability of simply supported 2D-FG cylindrical shells under combined loading and using the GDQ method are derived. Derivations are based on the classical shell theory and the power form composition of the constituent materials. The buckling analysis of such shells under different types of mechanical loads is investigated. It is concluded that:

1. The critical buckling loads of 2D-FG cylindrical shells are higher than 1D-FG cylindrical shells.
2. The critical buckling loads of a 2D-FG cylindrical shell under combined loading decline when power law index in z direction increases, when $n_x = 1$.
3. The critical buckling load decreases for 2D-FG cylindrical shell under combined loadings when the load parameter increases.
4. The more the R/h ratio, the less the critical buckling load of 2D-FG cylindrical shell under combined loading.
5. The more the L/R ratio, the less the critical buckling load of 2D-FG cylindrical shell under combined loading.

References

[1] M. YAMANOUCHI, M. KOIZUMI, T. HIRAI AND I. SHIOTA, Functionally Gradient Materials, Proc. First Int. Sympos, Japan, 1990.

[2] M. KOIZUMI, *Functionally gradient materials*, The Concept of FGM. Ceramic Trans., 34 (1993), pp. 3–10.

[3] D. O. BRUSH AND B. O. ALMORTH, Buckling of Bars, Plates and Shells, New York, McGraw-Hill, 1975.

[4] T. VODENITCHAROVA AND P. ANSOURIAN, *Buckling of circular cylindrical shells subjected to uniform lateral pressure*, J. Eng. Struct., 18(8) (1996), pp. 604–614.

[5] P. KHAZAEINEJAD, M. M. NAJAFIZADEH, J. JENABI AND M. R. ISVANDZIBAEI, *On the buckling of functionally graded cylindrical shells under combined external pressure and axial compression*, Int. J. Pressure Vessel Tech., 132 (2010).
[6] M. NEMAT-ALLA, *Reduction of thermal stresses by developing two dimensional functionally graded materials*, Int. J. Solids Struct., 40 (2003), pp. 7339–7356.
[7] R. S. DHALIWAL AND B. M. SINGH, *On the theory of elasticity of a non-homogenous medium*, J. Elast., 8 (1978), pp. 211–219.
[8] B. SOBHANI ARAGH AND H. HEDAYATI, *Static response and free vibration of two-dimensional functionally graded metal/ceramic open cylindrical shells under various boundary conditions*, Acta Mech., 223(2) (2012), pp. 309–330.
[9] M. J. PINDERA AND J. ABOUDI, *HOTCFGM-2D: HOTCFGM-2D: A coupled higher-order theory for cylindrical structural components with bi-directionally components with bi-directionally graded microstructures*, Final Report for NASA (Glenn Research Center), 2000, ID: 20000121257.
[10] M. ASGARI, M. AKHLAGHI AND M. HOSSEINI, *Dynamic analysis of two-dimensional functionally graded thick hollow cylinder with finite length under impact loading*, Acta Mech., 208 (2009), pp. 163–180.
[11] C. SHU C, Differential Quadrature and Its Application in Engineering, Berlin, Springer, 2000.
[12] S. SURESH AND A. MORTENSEN, Fundamentals of Functionally Graded Materials, London, IOM Comunications Ltd, 1998.
[13] J. N. REDDY, Mechanics of Laminated Composite Plates and Shells: Theory and Analysis, Boca Raton, CRC Press LLC; 2004.
[14] M. H. KARGARNOVIN AND M. SHAHSANAMI, *Buckling analysis of a composite cylindrical shell with fiber's material properties changing lengthwise using first-order shear deformation theory*, Shiraz, IRAN: Int Conf Mechanical Engineering, 2012.
[15] H. S. SHEN, *Post-buckling analysis of loaded functionally graded cylindrical shells in thermal environments*, J. Eng. Struct., 25(4) (2003), pp. 487–497.
[16] A. V. SOFIYEV, *Vibration and stability of composite cylindrical shells containing a fg layer subjected to various loads*, J. Struct. Eng. Mech., 27(3) (2007), pp. 365–391.
[17] A. R. RAHMANI, Thermal and Mechanical Buckling of Short and Long FG Cylindrical Shells Based on Some Variety Theory of the Shells, Department of Mechanical Engineering, Islamic Azad university, Arak Branch, Arak, IRAN: Final Thesis, 2007.